Original Article | Neuroimaging and Head & Neck

eISSN 2005-8330
https://doi.org/10.3348/kjr.2020.1201
Korean J Radiol 2021;22(8):1352-1368

Korean Journal of Radiology
KJR

Application of T1 Map Information Based on Synthetic MRI for Dynamic Contrast-Enhanced Imaging: A Comparison Study with the Fixed Baseline T1 Value Method

Dong Jae Shin[1], Seung Hong Choi[1, 2, 3], Roh-Eul Yoo[1], Koung Mi Kang[1], Tae Jin Yun[1], Ji-Hoon Kim[1], Chul-Ho Sohn[1], Sang Won Jo[4], Eun Jung Lee[5]

[1]Department of Radiology, Seoul National University College of Medicine, Seoul, Korea; [2]Center for Nanoparticle Research, Institute for Basic Science, Seoul, Korea; [3]School of Chemical and Biological Engineering, Seoul National University, Seoul, Korea; [4]Department of Radiology, Hallym University Dongtan Sacred Heart Hospital, Hwaseong, Korea; [5]Department of Radiology, Human Medical Imaging & Intervention Center, Seoul, Korea

Objective: For an accurate dynamic contrast-enhanced (DCE) MRI analysis, exact baseline T1 mapping is critical. The purpose of this study was to compare the pharmacokinetic parameters of DCE MRI using synthetic MRI with those using fixed baseline T1 values.

Materials and Methods: This retrospective study included 102 patients who underwent both DCE and synthetic brain MRI. Two methods were set for the baseline T1: one using the fixed value and the other using the T1 map from synthetic MRI. The volume transfer constant (K^{trans}), volume of the vascular plasma space (v_p), and the volume of the extravascular extracellular space (v_e) were compared between the two methods. The interclass correlation coefficients and the Bland-Altman method were used to assess the reliability.

Results: In normal-appearing frontal white matter (WM), the mean values of K^{trans}, v_e, and v_p were significantly higher in the fixed value method than in the T1 map method. In the normal-appearing occipital WM, the mean values of v_e and v_p were significantly higher in the fixed value method. In the putamen and head of the caudate nucleus, the mean values of K^{trans}, v_e, and v_p were significantly lower in the fixed value method. In addition, the T1 map method showed comparable interobserver agreements with the fixed baseline T1 value method.

Conclusion: The T1 map method using synthetic MRI may be useful for reflecting individual differences and reliable measurements in clinical applications of DCE MRI.

Keywords: *Magnetic resonance imaging; Perfusion imaging; Synthetic imaging; Dynamic contrast-enhanced MRI*

Received: October 09, 2020 **Revised:** December 13, 2020 **Accepted:** December 31, 2020

This study was supported by a grant from the Korea Healthcare technology R&D Projects, Ministry for Health, Welfare & Family Affairs (HI16C1111), by the Brain Research Program through the National Research Foundation of Korea (NRF) funded by the Ministry of Science, ICT & Future Planning (NRF-2016M3C7A1914002), by Basic Science Research Program through the National Research Foundation of Korea (NRF) funded by the Ministry of Science, ICT & Future Planning (NRF-2020R1A2C2008949 and NRF-2020R1A4A1018714), by Creative-Pioneering Researchers Program through Seoul National University (SNU), and by the Institute for Basic Science (IBS-R006-A1).

Corresponding author: Seung Hong Choi, MD, PhD, Department of Radiology, Seoul National University College of Medicine, Center for Nanoparticle Research, Institute for Basic Science, and School of Chemical and Biological Engineering, Seoul National University, 101 Daehak-ro, Jongno-gu, Seoul 03080, Korea.
• E-mail: verocay@snuh.org

Korean Journal of Radiology
KJR

INTRODUCTION

Dynamic contrast-enhanced (DCE) MRI is a noninvasive imaging technique for assessing microcirculation physiology and is relevant when studying a wide range of diseases and conditions. DCE MRI uses rapid T1-weighted image (T1WI) to measure the relaxation changes that result from gadolinium leakage into and out of the extravascular extracellular space and allows for the assessment of hemodynamic information, representing the vessel permeability, perfusion, and blood volume [1,2]. DCE MRI can be used to analyze the quantitative pharmacokinetic parameters that reflect the microcirculatory environment in imaged tissues. volume transfer constant (K^{trans}) is the volume transfer constant between the blood plasma and the extravascular extracellular space, volume of extravascular extracellular space (v_e) is the volume of extravascular extracellular space per unit volume of tissue and is also called the leakage space, and volume of vascular plasma space (v_p) is the volume of vascular plasma space per unit volume of tissue [3]. For an accurate DCE MRI analysis, it is important to obtain exact pharmacokinetic parameters, and in order to obtain these exact parametric values, accurate baseline T1 mapping is critical. Various imaging techniques for T1 mapping have been described in the literature, such as the variable flip angle technique, inversion recovery technique, and the look-locker technique [4-6]. However, these techniques are not robust, so recently, a fixed T1 value has been more widely used [7,8]. Nonetheless, the fixed T1 method has limitations in terms of accurately measuring the DCE parameters because every tissue is set at the same value [9].

Synthetic MRI is a technique based on the quantification of physical tissue properties. This technique uses a multi-echo and multi-delay acquisition method that quantifies the longitudinal T1 and transverse T2 relaxation times and proton density. By manipulating the acquisition parameters, including the repetition time (TR), echo time (TE), and inversion time, a single acquisition can generate multiple sequences and obtain a precise T1 value for each pixel [10-12]. Synthetic MRIs have already been used for relaxation measurements [13,14], and their accuracy and reproducibility have been demonstrated in repeated phantom measurements [15]. The previously proposed T1 measurement methods are known to have limitations, including low reproducibility and long scan time [16]. Our proposed T1 map method based on synthetic MRI could overcome these limitations, which have a reasonable scan time and reproducible measurement.

To the best of our knowledge, there have been no previous reports regarding the application of baseline T1 mapping from synthetic MRI for DCE MRI analysis. The purpose of the present study was to compare the pharmacokinetic parameters of DCE MRI using synthetic MRI with those using the fixed baseline T1 values and the interobserver agreements in the DCE parameters between these two methods.

MATERIALS AND METHODS

The Institutional Review Board of Seoul National University Hospital approved this retrospective study and waived the informed consent requirement (IRB No. H-1803-137-933).

Patients

We retrospectively enrolled 102 consecutive patients who had undergone both DCE and synthetic MRI from September 2016 to June 2017 (32 male, 70 female; mean age, 62.65 years; age range, 22–87 years) for the further evaluation of clinically suspected white matter (WM) disease or neurological disorders. Final diagnoses included migraine (33%), small vessel disease (19%), other headaches (10%), infarctions (8%), dementia (5%), and other diagnoses (26%).

Image Acquisition

All brain imaging was performed on a 3T MRI system (Discovery MR 750; GE Healthcare) using a 32-channel phased array head coil. All patients underwent a synthetic MR sequence (multi-dynamic multi-echo sequence; MDME sequence) and a DCE MR sequence in addition to conventional MR sequences.

The MDME sequence data were acquired before injection of the contrast agent. The data include four automatically calculated saturation delays and two TEs (21.4 msec and 85.4 msec), and a TR of 4000 msec. The MDME data were reconstructed using a vendor-provided program (SyMRI 7.2; Synthetic MR), and quantitative T1 maps were generated. The parameters used for the quantitative T1 map were: field of view, 240 x 240 mm; matrix, 320 x 256; echo-train length, 12; bandwidth, 22.73 kHz; slice thickness/gap, 4.0 mm/1.0 mm; number of slices, 20; and a total acquisition time of 5 minutes and 8 seconds.

 https://doi.org/10.3348/kjr.2020.1201

DCE MRI was performed using a 3D gradient-echo T1WI after intravenous administration of gadobutrol (Gadovist, Bayer Schering Pharma) (0.1 mmoL/kg body weight) using a power injector (Spectris, MedRad) at a rate of 4 mL/s. A 30 mL bolus injection of saline followed the gadobutrol treatment at the same injection rate. For each section, 40 slices per patient were acquired at intervals equal to the TR. The following MR parameters were used: TR, 2.8 msec; TE, 1.0 msec; flip angle, 10°; and matrix, 128 x 128 with a section thickness of 3 mm, a field of view of 249 x 249 mm, a voxel size of 1.25 x 1.25 x 3 mm^3, a pixel bandwidth of 789 Hz, and a total acquisition time of 5 minutes and 25 seconds.

Image Analysis

In all 102 patients, the DCE parameters were measured in the normal-appearing frontal and occipital WM, putamen, and head of caudate nucleus. We then measured the DCE parameters of the high signal intensity areas on fluid attenuated inversion recovery (FLAIR) imaging in the frontal and occipital WM in 78 and 66 patients, respectively, which did not show any visual contrast enhancement on the contrast-enhanced T1WI. DCE MRI analysis was performed using a dedicated software package (NordicICE 4.1.1, NordicNeuroLab). In the DCE analysis, we used two methods for setting the baseline T1: one using the fixed value and the other using the T1 map from the synthetic MRI. The

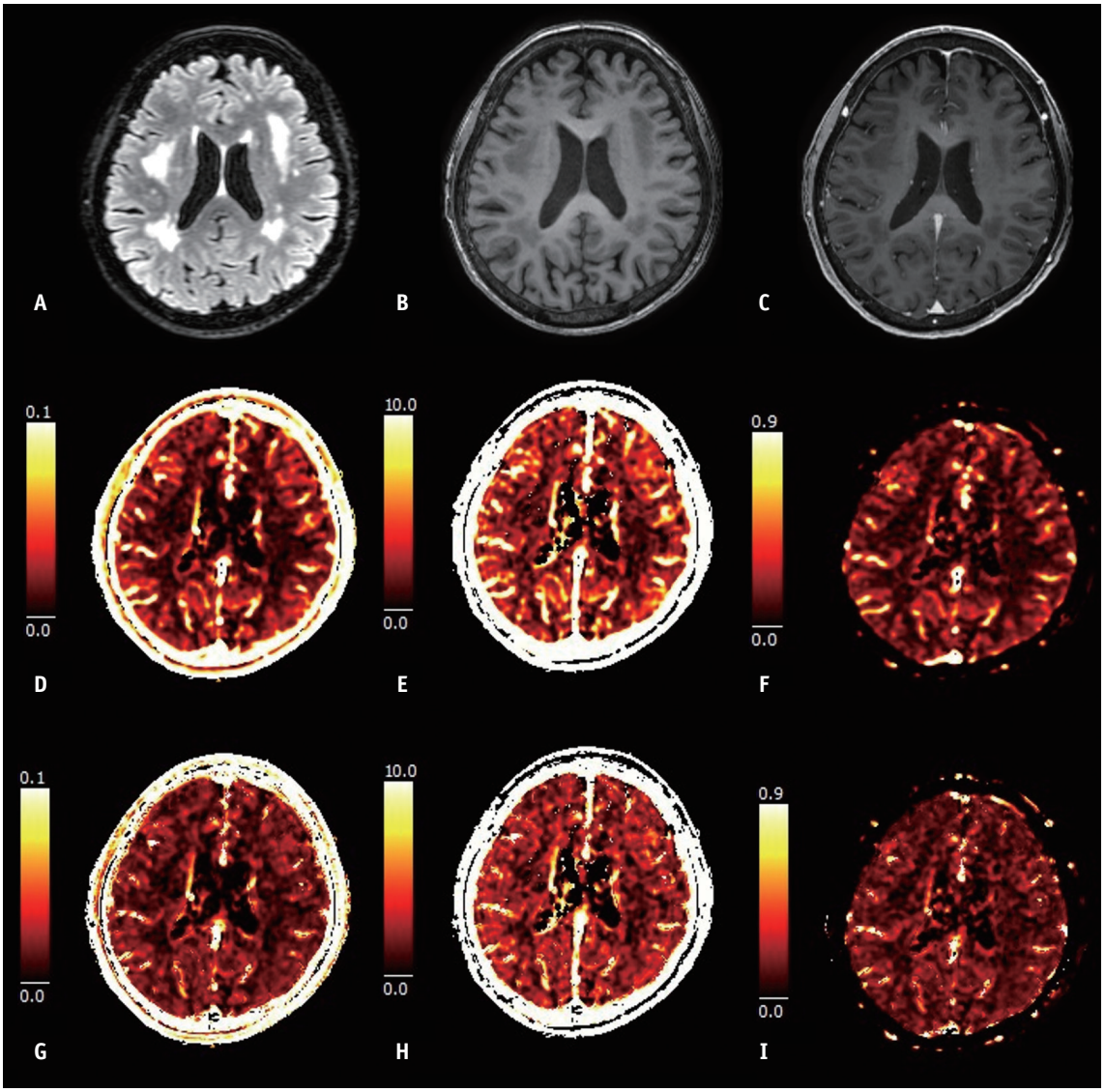

Fig. 1. Pharmacokinetic parametric maps.
A. Fluid attenuated inversion recovery. **B.** Precontrast. **C.** Post T1-weighted images. **D.** K^{trans}. **E.** v_e. **F.** v_p maps obtained by the fixed value method. **G.** K^{trans}. **H.** v_e. **I.** v_p maps obtained by the T1 map method using synthetic MRI. K^{trans} = volume transfer constant, v_e = volume of extravascular extracellular space, v_p = volume of vascular plasma space

https://doi.org/10.3348/kjr.2020.1201

Korean Journal of Radiology
KJR

fixed baseline T1 values were determined by averaging the results of the T1 relaxation time reported in several studies [17-20]. The averaging results of each region are as follows: frontal WM, 795 ms; occipital WM, 795 ms; putamen, 1257 ms; and head of caudate nucleus, 1379 ms. In the T1 map, the quantitative T1 map obtained from the synthetic MRI was used. Coregistration between the DCE MRI and the quantitative T1 map was performed automatically using the dedicated software package. For the arterial input function (AIF), a population-based AIF was determined using NordicICE. On the basis of the extended Tofts model, the perfusion analysis method was used to calculate pharmacokinetic parameters, including K^{trans}, v_e, and v_p (Fig. 1). Owing to the differences in the slice number and thickness between the FLAIR images and parametric maps, the FLAIR images were resampled automatically based on the pharmacokinetic maps. One neuroradiologist (observer 1) (with 8 years of brain MRI experience) drew regions of interest (ROIs) in both the normal-appearing and high signal intensity areas in the occipital and frontal WM on the resampled FLAIR images in each patient. ROIs were also drawn in the putamen, and the head of caudate nucleus, where no abnormal signal changes were observed (Fig. 2). The average size of all ROIs was approximately 0.7 cm^2. Finally, in each ROI, the mean parametric values from the DCE MRI were obtained using both the fixed value method and the T1 map method (Fig. 3). The other neuroradiologist (observer 2) measured the parametric values in an identical way to evaluate the interobserver agreement (with 16 years of experience in brain MRI).

Statistical Analysis

All statistical analyses were performed using SPSS, version 19 (IBM Corp.) or MedCalc statistical software, version 18 (MedCalc). *p* values less than 0.05 were considered statistically significant.

We compared the mean values of the pharmacokinetic parameters, including K^{trans}, v_e, and v_p, from the DCE MRI between the fixed value method and the T1 map method using paired *t* tests (SPSS). To compare the differences in the pharmacokinetic parameters between normal-appearing WM and high signal intensity areas in WM on FLAIR imaging, paired *t* tests were also used (MedCalc). We assessed the interobserver reproducibility by using the interclass correlation coefficient (ICC) and the Bland-Altman plot (MedCalc). The interobserver assessment was defined as a comparison between the measurements from observers 1 and 2. All values of the pharmacokinetic parameters were assessed. The ICC values were categorized as follows: < 0.40, poor; 0.40–0.59, fair; 0.60–0.74, good; and > 0.74, excellent. We also correlated the T1 and pharmacokinetic values based on the T1 map method with age and sex, which are given in the online appendix (SPSS).

RESULTS

Comparison of the T1 Values and the Pharmacokinetic Parameters between the Fixed Value and T1 Map Method

The comparison results between the mean T1 values in the literature and mean T1 values from the synthetic MRI are shown in Table 1. In the normal-appearing occipital

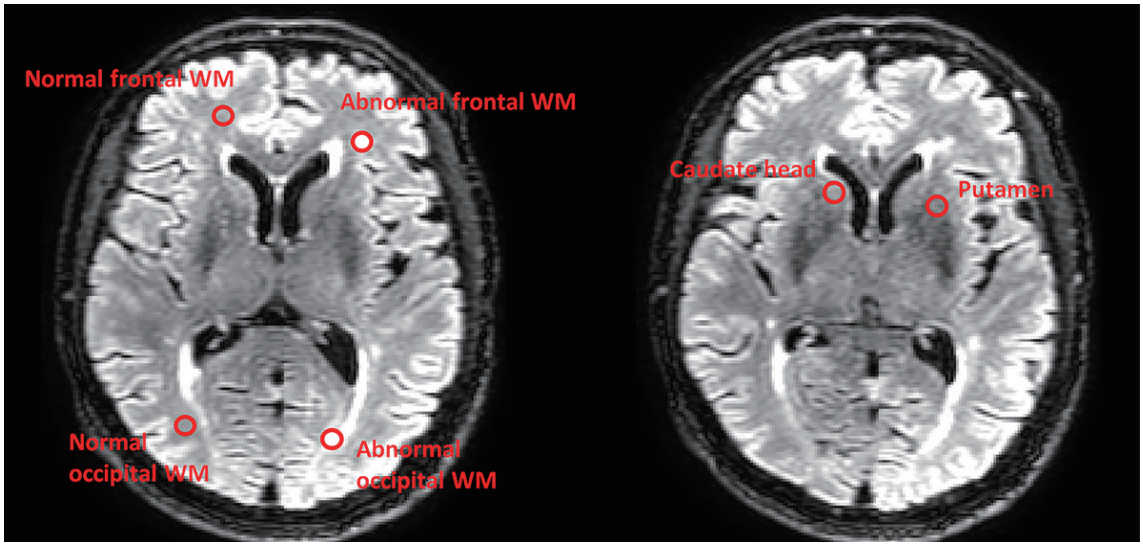

Fig. 2. Resampled fluid attenuated inversion recovery images based on the parametric maps. The regions of interest are located in the six areas. WM = white matter

https://doi.org/10.3348/kjr.2020.1201

WM, putamen, and head of caudate nucleus, the mean T1 values from the synthetic MRI were significantly lower than the mean T1 values in the literature.

The comparison results between the mean parametric values using a fixed baseline T1 value and a T1 map using synthetic MRI are shown in Table 2. In the normal-

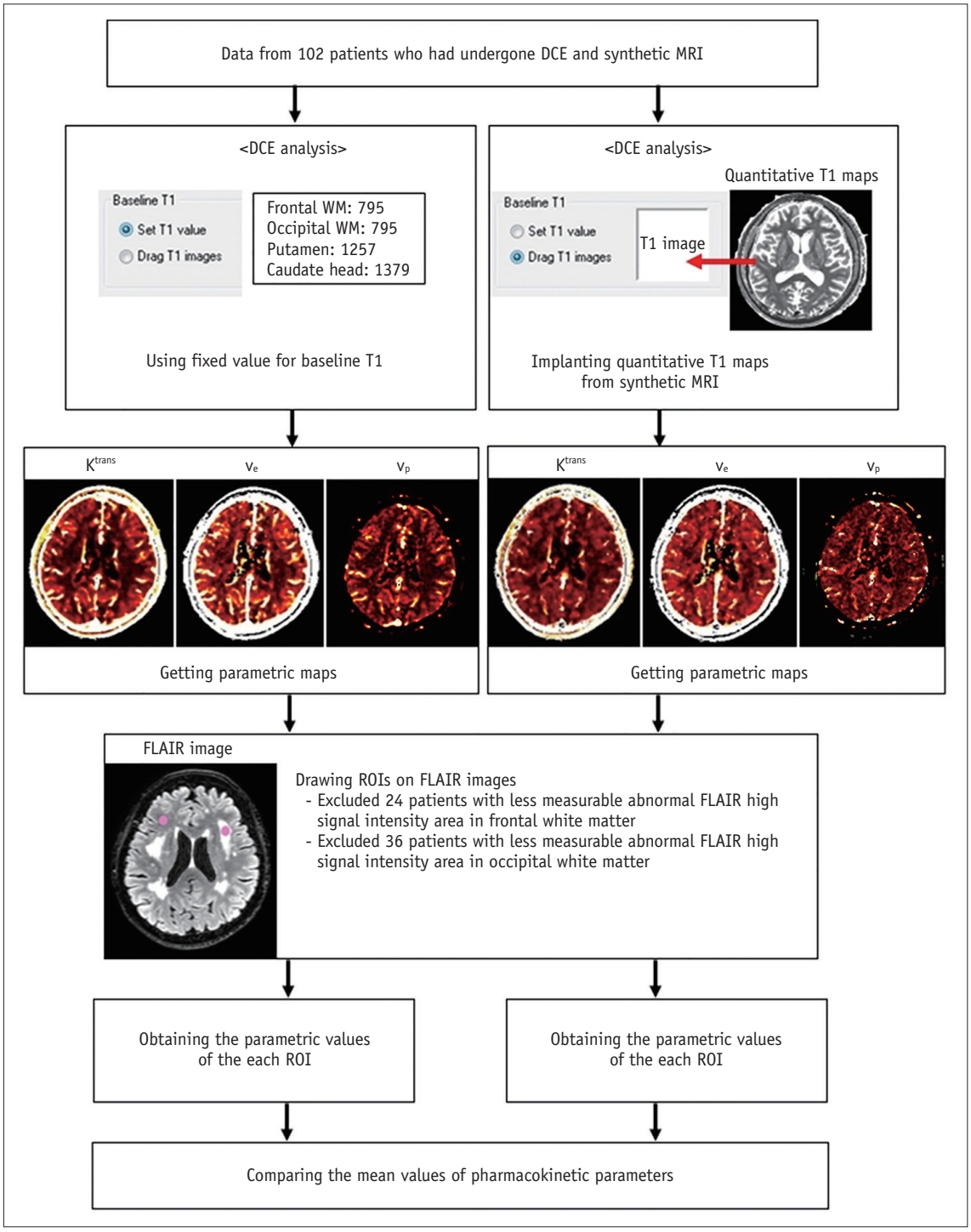

Fig. 3. Flowchart of the study. The fixed T1 values were used according to the brain areas where the ROIs were drawn, which is available by using the dedicated software package. For example, when a ROI was drawn on the frontal WM and putamen, we used a fixed T1 value of 795 and 1257 msec, respectively, for the measurement of the permeability values. DCE = dynamic contrast-enhanced, FLAIR = fluid attenuated inversion recovery, K^{trans} = volume transfer constant, ROI = region of interest, v_e = volume of extravascular extracellular space, v_p = volume of vascular plasma space, WM = white matter

https://doi.org/10.3348/kjr.2020.1201

Korean Journal of Radiology
KJR

Table 1. The Mean T1 Values in the Literatures and from Synthetic MRI

	Mean T1 Values in the Literatures	Mean T1 Values from Synthetic MRI	Difference*	Mean Difference (%)†	*P*
Normal-appearing frontal WM	795	787	8	1.0	0.101
Normal-appearing occipital WM	795	766	29	3.6	< 0.001
Putamen	1257	1116	141	11.2	< 0.001
Head of caudate nucleus	1379	1112	267	19.4	< 0.001

*Difference = T1 values in the literature - T1 values from synthetic MRI, †Mean difference = difference/T1 values in the literature x 100. WM = white matter

Table 2. Pharmacokinetic Parameters Obtained with the Fixed Value Method and the T1 Map Method Using Synthetic MRI

Pharmacokinetic Parameters	Fixed Value Method	T1 Map Method	Difference*	Mean Difference (%)†	*P*
Normal-appearing frontal WM					
K^{trans}	0.0139	0.0114	0.0025	17.99	< 0.001
v_e	4.2078	3.6195	0.5883	13.98	< 0.001
v_p	0.2151	0.1737	0.0414	19.24	0.001
Normal-appearing occipital WM					
K^{trans}	0.0191	0.0193	0.0002	1.04	0.949
v_e	5.7348	5.0269	0.7079	12.34	0.002
v_p	0.1969	0.1715	0.0254	12.90	0.001
High signal intensity areas in frontal WM					
K^{trans}	0.0173	0.0133	0.0040	23.12	< 0.001
v_e	8.3140	9.3860	1.0720	12.89	0.712
v_p	0.1653	0.1220	0.0433	26.19	< 0.001
High signal intensity areas in occipital WM					
K^{trans}	0.0121	0.0093	0.0028	23.14	< 0.001
v_e	5.1713	3.8081	1.3632	26.36	0.012
v_p	0.1353	0.1080	0.0273	20.18	< 0.001
Putamen					
K^{trans}	0.0190	0.0269	-0.0079	-41.58	< 0.001
v_e	5.5087	7.2278	-1.7191	-31.21	< 0.001
v_p	0.4383	0.6665	-0.2282	-52.06	0.008
Head of caudate nucleus					
K^{trans}	0.0121	0.0169	-0.0048	-39.67	< 0.001
v_e	3.3325	4.5898	-1.2573	-37.73	< 0.001
v_p	0.2106	0.3050	-0.0944	-44.82	0.009

Units of K^{trans} = min^{-1}. *Difference = fixed value method - T1 map method, †Mean difference = difference/fixed value method x 100. K^{trans} = volume transfer constant, v_e = volume of extravascular extracellular space, v_p = volume of vascular plasma space, WM = white matter

appearing frontal WM, the mean values of K^{trans}, v_e, and v_p were significantly higher in the fixed value method than in the T1 map method. In the normal-appearing occipital WM, the mean values of v_e and v_p were significantly higher in the fixed value method than in the T1 map method. In the putamen and head of caudate nucleus, the mean values of K^{trans}, v_e, and v_p were significantly lower in the fixed value method than in the T1 map method. In the high signal intensity areas of the frontal WM on FLAIR images, the mean values of K^{trans} and v_p were significantly higher in the fixed value method than in the T1 map method. In the high signal intensity areas of the occipital WM on FLAIR images, the mean values of K^{trans}, v_e, and v_p were significantly higher in the fixed value method than in the T1 map method. In terms of the comparison of the pharmacokinetic parameters between the fixed value and T1 map method, the box-and-whisker graphs and dot-and-line diagrams for the pharmacokinetic parameters are shown in Figure 4, and the Bland-Altman plots are shown in Figure 5.

https://doi.org/10.3348/kjr.2020.1201

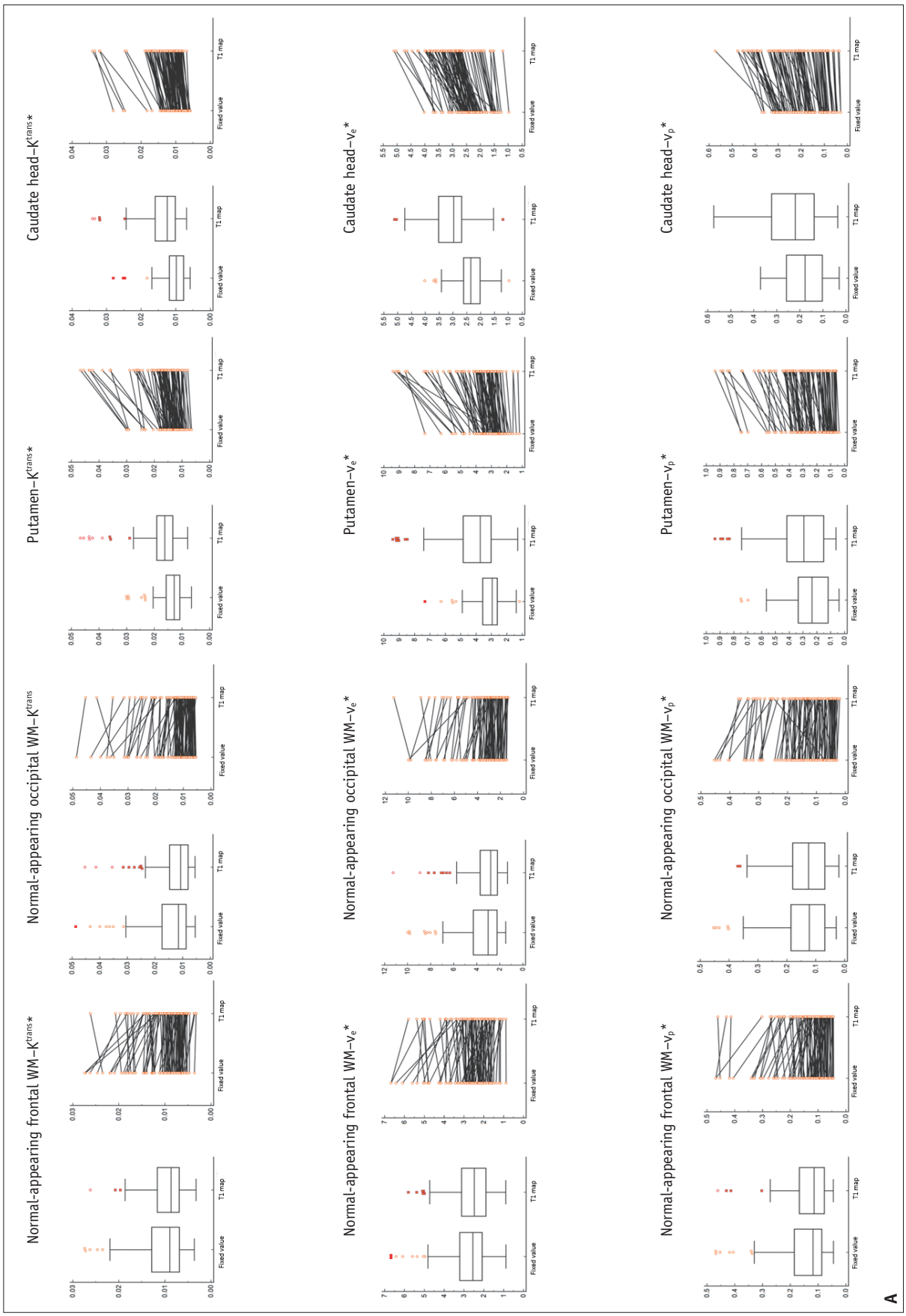

Fig. 4. Box-whisker plots and dot-and-line diagrams showing the pharmacokinetic parametric values of the two methods in the normal-appearing areas (A) and high SI areas (B). Lines in boxes = median values. Boundaries of boxes = 25th and 75th percentiles, with whiskers extending from the median to ± 1.5 x interquartile ranges and outliers beyond the whiskers denoted by points. Statistically significant results are marked with asterisks. K^{trans} = volume transfer constant, SI = signal intensity, v_e = volume of extravascular extracellular space, v_p = volume of vascular plasma space, WM = white matter

https://doi.org/10.3348/kjr.2020.1201

Korean Journal of Radiology
KJR

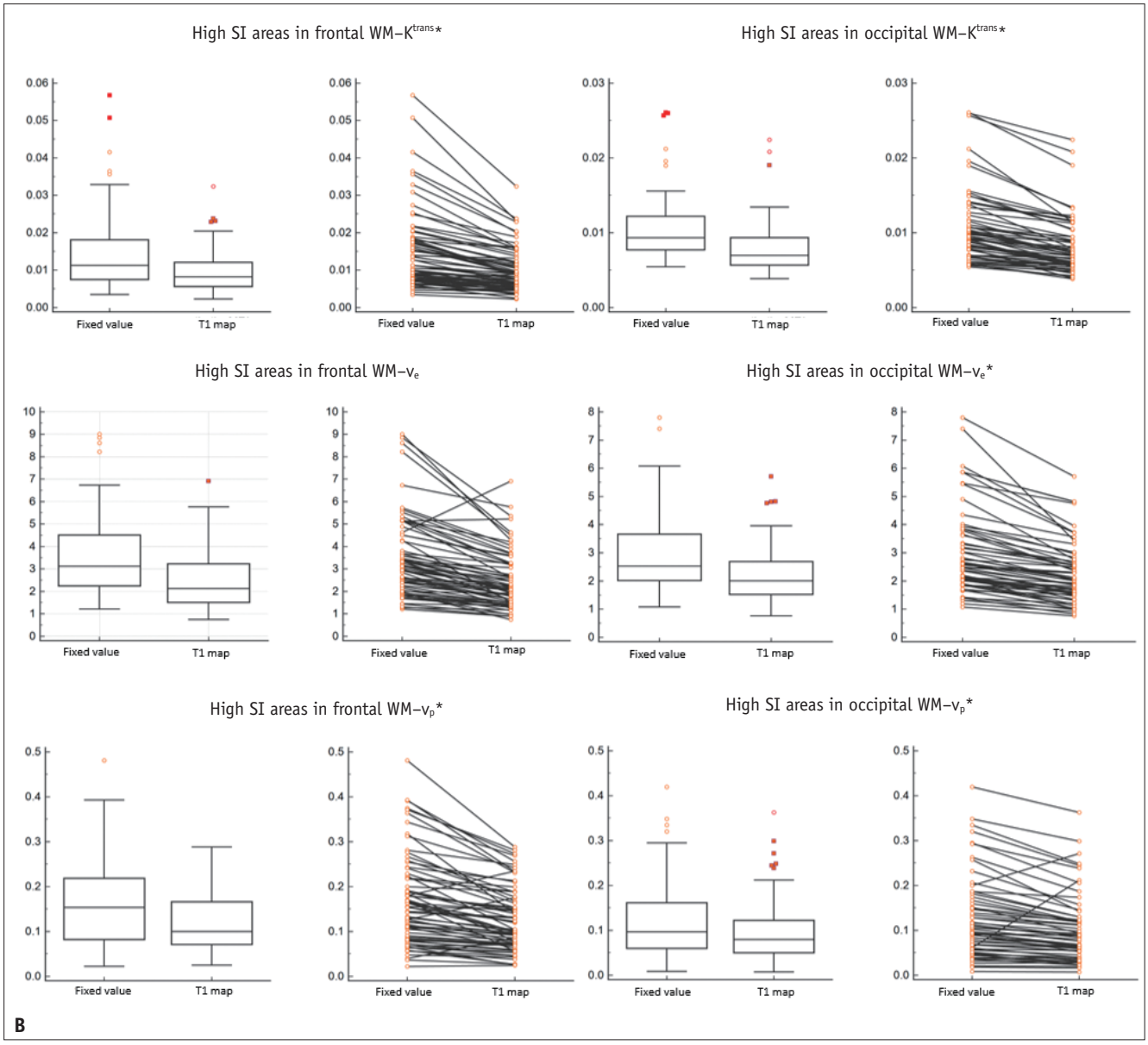

Fig. 4. Box-whisker plots and dot-and-line diagrams showing the pharmacokinetic parametric values of the two methods in the normal-appearing areas (A) and high SI areas (B). Lines in boxes = median values. Boundaries of boxes = 25th and 75th percentiles, with whiskers extending from the median to ± 1.5 x interquartile ranges and outliers beyond the whiskers denoted by points. Statistically significant results are marked with asterisks. K^{trans} = volume transfer constant, SI = signal intensity, v_e = volume of extravascular extracellular space, v_p = volume of vascular plasma space, WM = white matter

Comparison of the Pharmacokinetic Parameters between the Normal-Appearing WM and High Signal Intensity Areas in the WM on FLAIR Imaging

The comparison results of the mean parametric values between the normal-appearing WM and high signal intensity areas in the WM on FLAIR imaging are shown in Table 3. In the frontal WM, the mean value of v_e was significantly higher in the high signal intensity area than in the normal-appearing area when only based on the fixed value methods. In addition, the mean values of v_p were significantly lower in the high signal intensity area than in the normal-appearing area when based on both fixed value and T1 map methods. In the occipital WM, the mean value of K^{trans} was significantly lower in the high signal intensity area than in the normal-appearing area when only based on the fixed value method. The mean values of v_p were significantly lower in the high signal intensity area than in the normal-appearing area when based on both fixed value

https://doi.org/10.3348/kjr.2020.1201

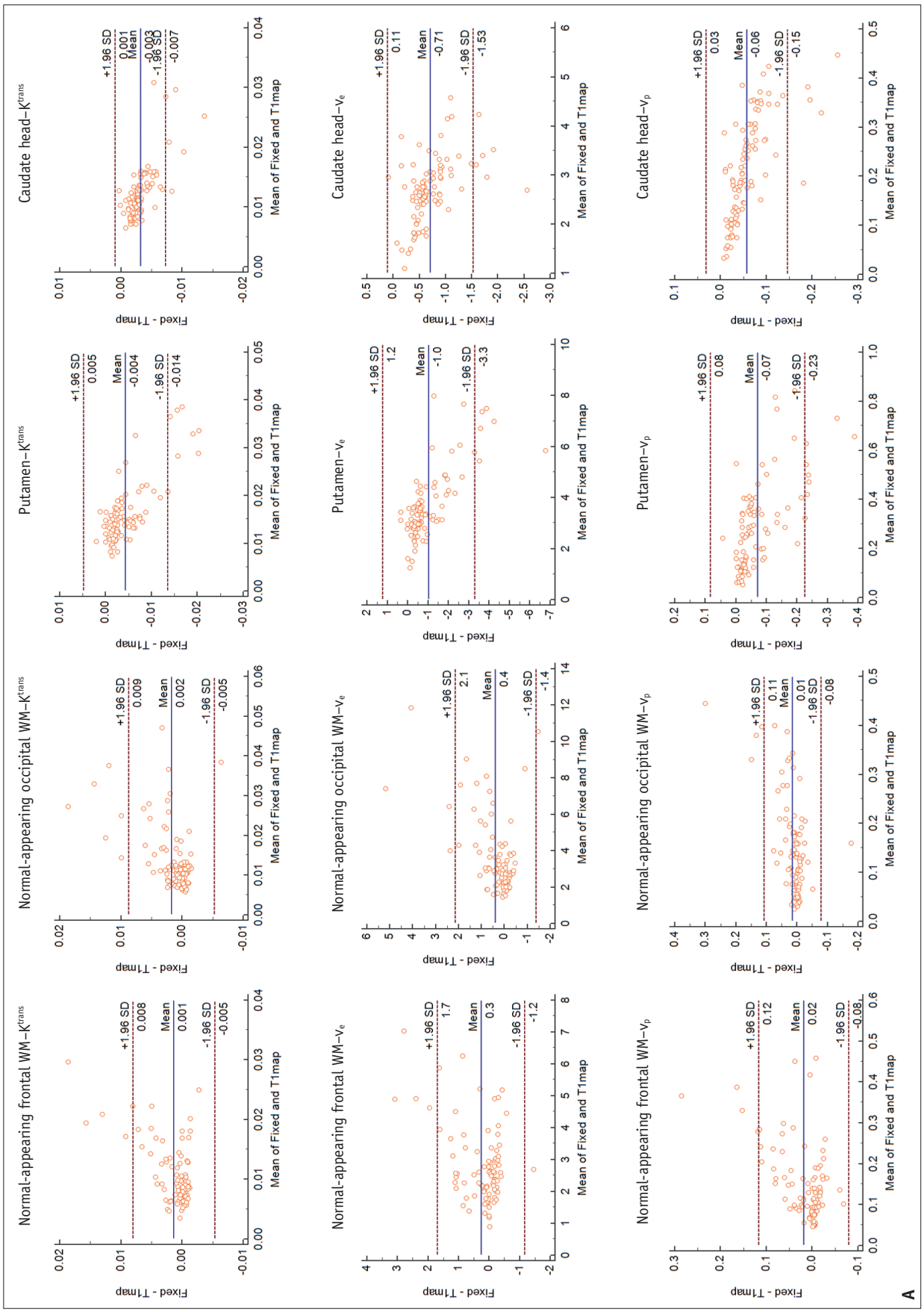

Fig. 5. Bland-Altman plots showing the comparison of the pharmacokinetic values between fixed value method and T1 map method in normal-appearing areas (A) and high signal intensity areas (B). Fixed = fixed value method, K^{trans} = volume transfer constant, SD = standard deviation, T1 map = T1 map method, v_e = volume of extravascular extracellular space, v_p = volume of vascular plasma space, WM = white matter

https://doi.org/10.3348/kjr.2020.1201

Korean Journal of Radiology
KJR

and T1 map methods. In all WM, the mean value of v_p was significantly lower in the high signal intensity area than in the normal-appearing area when only based on the T1 map method.

Interobserver Reproducibility of the Fixed Value and T1 Map Method

Interobserver reproducibility revealed an ICC that showed similar reproducibility between the two methods (Table 4).

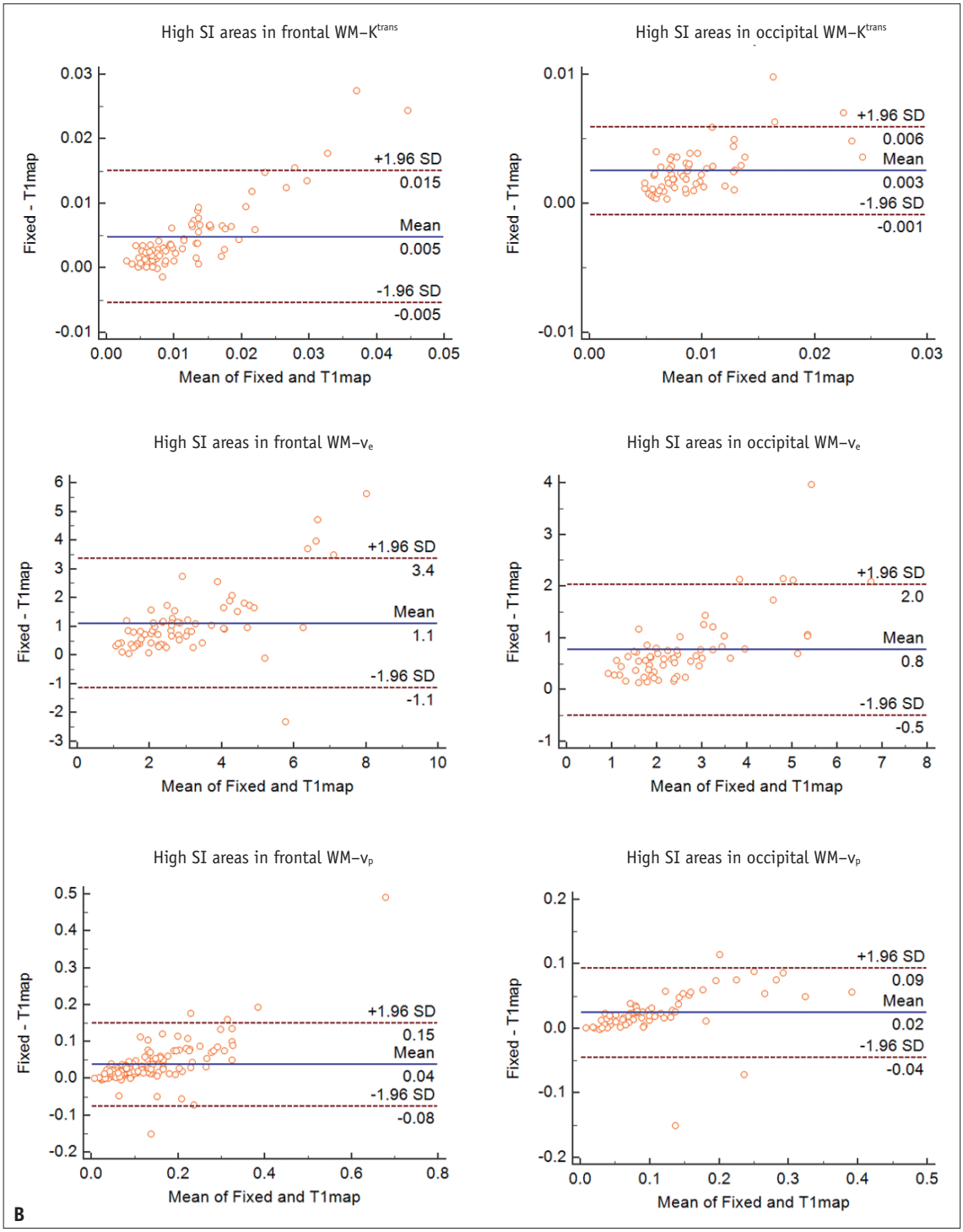

Fig. 5. Bland-Altman plots showing the comparison of the pharmacokinetic values between fixed value method and T1 map method in normal-appearing areas (A) and high signal intensity areas (B). Fixed = fixed value method, K^{trans} = volume transfer constant, SD = standard deviation, T1 map = T1 map method, v_e = volume of extravascular extracellular space, v_p = volume of vascular plasma space, WM = white matter

https://doi.org/10.3348/kjr.2020.1201

Table 3. Comparison of the Pharmacokinetic Parameters between the Normal-Appearing WM and the High Signal Intensity Areas in the WM

Pharmacokinetic Parameters	Normal-Appearing Areas	High Signal Intensity Areas	Difference*	Mean Difference (%)†	*P*
Frontal WM					
Fixed value method					
K^{trans}	0.0152	0.0173	-0.0021	-13.82	0.431
v_e	4.4484	8.3140	-3.8656	-86.90	0.048
v_p	0.2391	0.1653	0.0738	30.87	0.005
T1 map method					
K^{trans}	0.0118	0.0133	-0.0015	-12.71	0.586
v_e	3.6670	9.3860	-5.7190	-155.96	0.129
v_p	0.1800	0.1220	0.0580	32.22	< 0.001
Occipital WM					
Fixed value method					
K^{trans}	0.0204	0.0121	0.0083	40.69	0.004
v_e	6.1912	5.1713	1.0199	16.47	0.570
v_p	0.2286	0.1353	0.0933	40.81	0.007
T1 map method					
K^{trans}	0.0518	0.0093	0.0125	24.13	0.064
v_e	5.4221	3.8081	1.6140	29.77	0.254
v_p	0.1776	0.1080	0.0696	39.19	< 0.001
All WM					
Fixed value method					
K^{trans}	0.0175	0.0149	0.0026	14.86	0.185
v_e	5.2472	6.8736	-1.6264	-30.99	0.226
v_p	0.2347	0.1907	0.0440	18.74	0.186
T1 map method					
K^{trans}	0.0163	0.0115	0.0048	29.44	0.157
v_e	4.4714	6.8295	-2.3581	-52.73	0.271
v_p	0.1819	0.1338	0.0481	26.44	0.011

Units of K^{trans} = min^{-1}. *Difference = normal-appearing WM - high signal intensity areas in WM, †Mean difference = difference/normal-appearing WM x 100. K^{trans} = volume transfer constant, v_e = volume of extravascular extracellular space, v_p = volume of vascular plasma space, WM = white matter

Excellent interobserver agreements were achieved in areas with high signal intensity of the normal-appearing occipital WM and high signal intensity areas in the occipital WM and head of the caudate nucleus. Except for the K^{trans} value in the high signal intensity areas in frontal WM, fair to excellent interobserver agreements were noted in areas of normal-appearing frontal WM, high signal intensity areas in frontal WM, and putamen. The results of the Bland-Altman plot revealed good agreement in both the fixed value and the T1 map methods for measuring the pharmacokinetic parameters, which are presented in Figure 6.

Correlations of the T1 Values based on T1 Map Method with Age and Sex

The comparison results between the T1 values based on the T1 map method and age are shown in Figure 7. The comparison results between the T1 values based on the T1 map method and sex are shown in Table 5.

DISCUSSION

This study compared the pharmacokinetic parameters of DCE MRI between the fixed value and T1 map methods. There were significant differences between the two methods. For WM, the DCE parameters tend to be lower in the T1 map method than in the fixed value methods, and vice versa for the head of caudate nucleus and putamen. In addition, the two methods showed similar interobserver agreements for the measurement.

The T1 relaxation time varies depending on the

https://doi.org/10.3348/kjr.2020.1201

Korean Journal of Radiology
KJR

Table 4. ICC for the Fixed Value Method and the T1 Map Method Using Synthetic MRI

Pharmacokinetic Parameters	Fixed Value Method	T1 Map Method
Normal-appearing frontal WM		
K^{trans}	0.590 (0.392 to 0.723)	0.574 (0.368 to 0.713)
v_e	0.690 (0.539 to 0.791)	0.728 (0.596 to 0.816)
v_p	0.535 (0.311 to 0.687)	0.632 (0.454 to 0.752)
Normal-appearing occipital WM		
K^{trans}	0.955 (0.929 to 0.971)	0.942 (0.908 to 0.963)
v_e	0.885 (0.819 to 0.927)	0.995 (0.991 to 0.997)
v_p	0.843 (0.752 to 0.900)	0.852 (0.766 to 0.906)
High signal intensity areas in frontal WM		
K^{trans}	0.400 (0.103 to 0.597)	0.288 (-0.063 to 0.523)
v_e	0.625 (0.430 to 0.753)	0.527 (0.282 to 0.689)
v_p	0.682 (0.527 to 0.786)	0.672 (0.512 to 0.779)
High signal intensity areas in occipital WM		
K^{trans}	0.817 (0.699 to 0.889)	0.865 (0.777 to 0.918)
v_e	0.770 (0.613 to 0.863)	0.821 (0.699 to 0.894)
v_p	0.788 (0.650 to 0.871)	0.794 (0.661 to 0.875)
Putamen		
K^{trans}	0.707 (0.565 to 0.803)	0.722 (0.584 to 0.814)
v_e	0.587 (0.373 to 0.728)	0.776 (0.651 to 0.856)
v_p	0.880 (0.818 to 0.920)	0.880 (0.817 to 0.921)
Caudate head		
K^{trans}	0.773 (0.662 to 0.847)	0.954 (0.932 to 0.969)
v_e	0.836 (0.754 to 0.890)	0.821 (0.732 to 0.881)
v_p	0.875 (0.813 to 0.916)	0.916 (0.875 to 0.944)

Values in parentheses indicate the 95% confidence interval. ICC = interclass correlation coefficient, K^{trans} = volume transfer constant, v_e = volume of extravascular extracellular space, v_p = volume of vascular plasma spac, WM = white matter

measurement method and each individual, even in the same region of the brain, which is one of the necessary values for measuring the pharmacokinetic parameters of DCE MRI. We believe that synthetic MRI has some benefits when measuring the T1 relaxation time of the brain. First, the T1 relaxation time is dependent on the field strength and pulse sequence. Lu et al. [19] reported that the T1 relaxation time was 14–30% longer at 3T when compared to the values at 1.5T. In another study, the T1 values were found to increase with field strength at 1.5, 3, and 7T [20]. They also reported that the values in the same 3T study differed depending on the pulse sequence used in the measurement. In contrast, synthetic MRI is a technique to stably obtain the absolute magnetic properties, such as the T1 relaxation times of the brain tissues, independent of the scanner settings [21]. Second, the T1 relaxation time is different for each individual, especially when considering age and sex. There are significant differences in the T1 relaxation times measured between female and male brains. According to Wansapura et al. [17], females have a longer T1 relaxation time than males in gray matter and WM areas. In addition, age is also a factor affecting the normal T1 relaxation time. Breger et al. [22] reported that the T1 values in the telencephalon tend to increase by approximately 0.1% per year. According to Steen et al. [23], T1 values generally increase with age, and brain aging is associated with occult processes that can begin at a relatively early age. Cho et al. [24] found that brain tissue continues to change throughout the lifespan among healthy subjects with no neurologic deficits. Age-related changes follow a remarkably different schedule in different brain tissues; WM tracts tend to reach a minimum T1 value and increase again earlier than gray matter tracts do. Thus, for the exact measurement of pharmacokinetic parameters in each brain region, such individual variations in T1 values should be considered. In each subject, we obtained reliable T1 relaxation times of the brain regions via synthetic MRI.

The multiple flip angle technique is the most widely used technique for baseline T1 measurement because it requires less acquisition time and thus is more attractive for clinical use. However, the technique has weak reproducibility due to motion artifacts and B1 field inhomogeneity. Although

 https://doi.org/10.3348/kjr.2020.1201

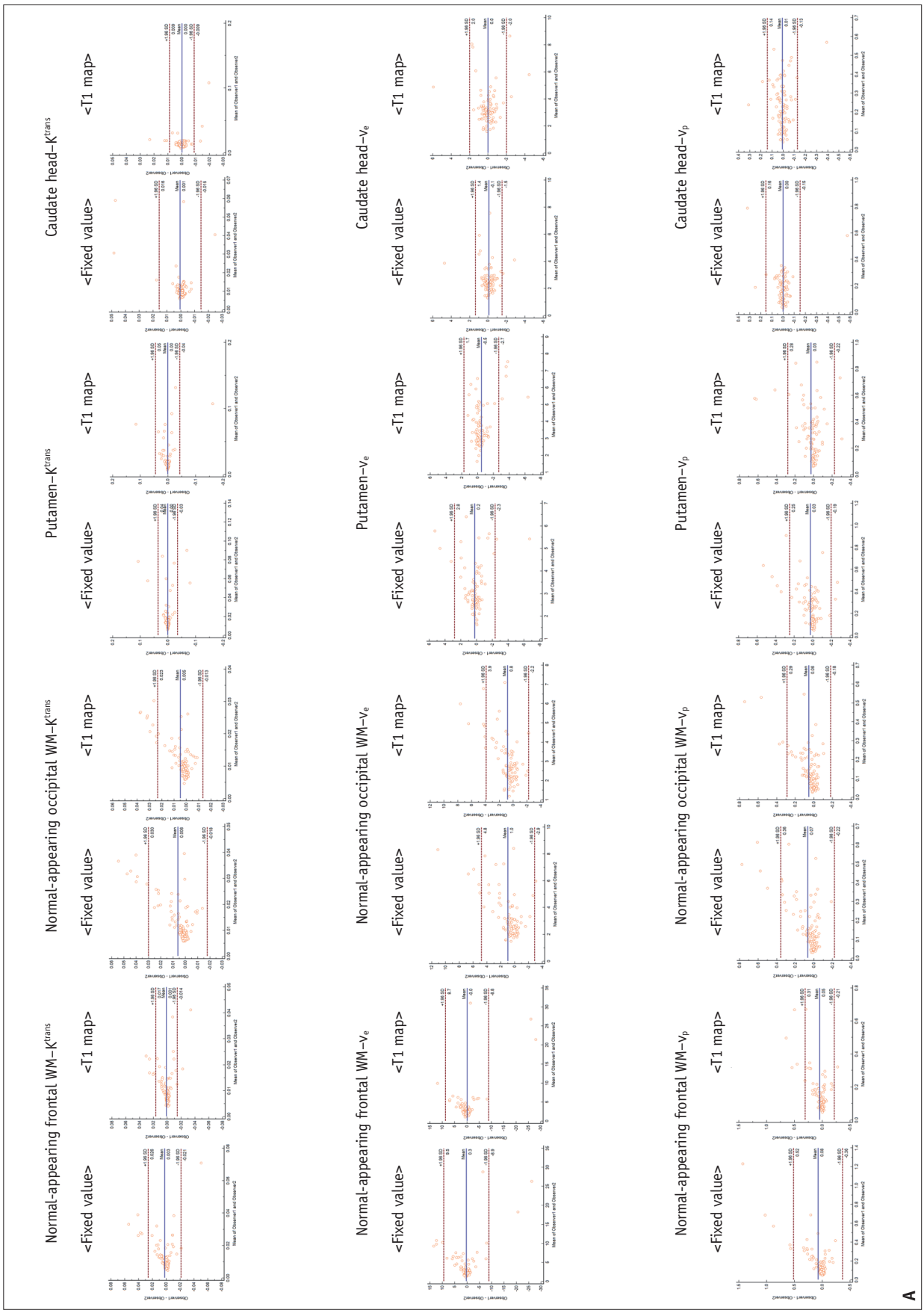

Fig. 6. Bland-Altman plots showing interobserver reproducibility between the measurements from observer 1 and observer 2 in normal-appearing areas (A) and high signal intensity areas (B). Between both measurements, 95% limits of agreement are similarly observed. Fixed value = fixed value method, K^{trans} = volume transfer constant, SD = standard deviation, T1 map = T1 map method, v_e = volume of extravascular extracellular space, v_p = volume of vascular plasma space, WM = white matter

https://doi.org/10.3348/kjr.2020.1201

Korean Journal of Radiology
KJR

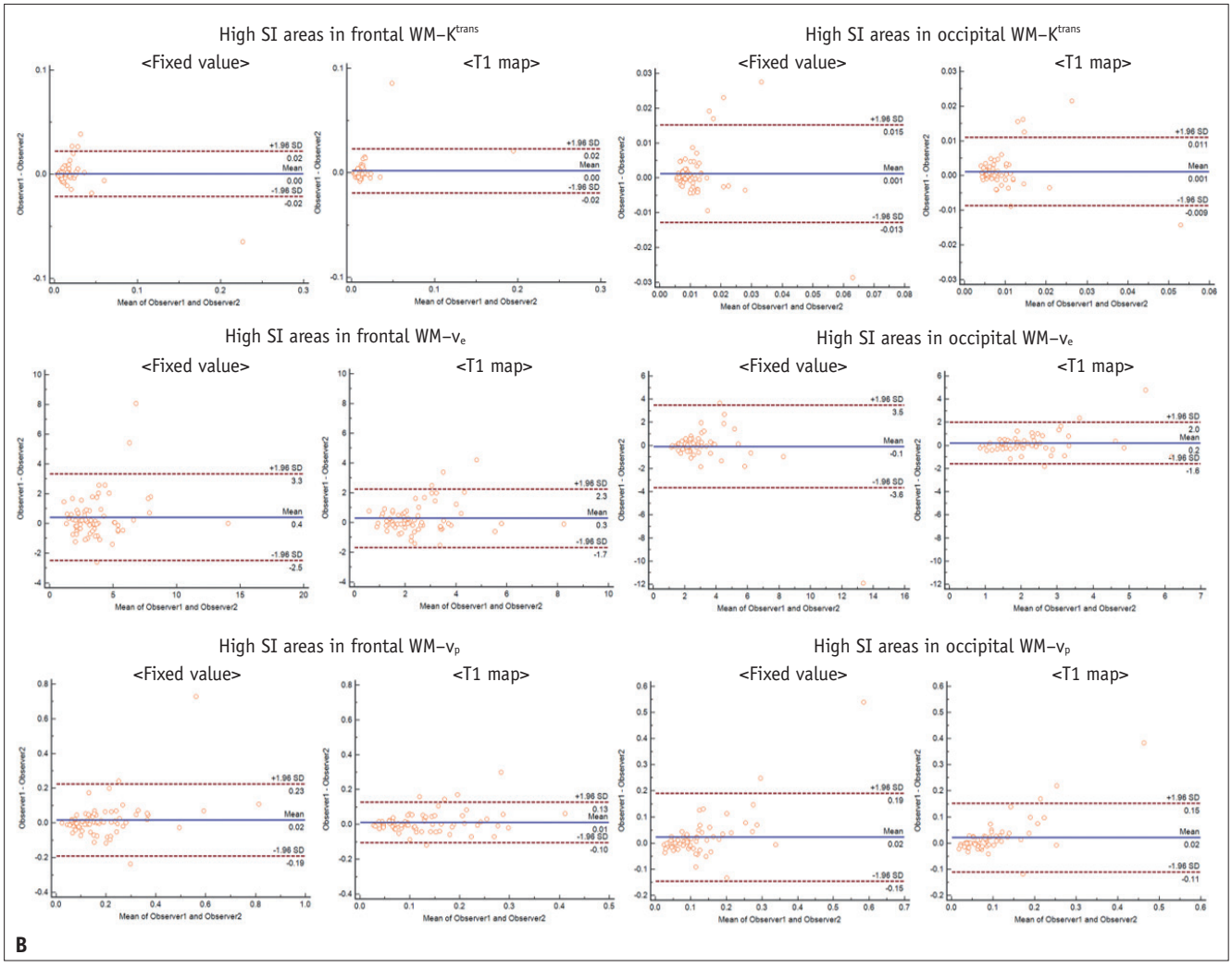

Fig. 6. Bland-Altman plots showing interobserver reproducibility between the measurements from observer 1 and observer 2 in normal-appearing areas (A) and high SI areas (B). Between both measurements, 95% limits of agreement are similarly observed. Fixed = fixed value method, K^{trans} = volume transfer constant, SD = standard deviation, SI = signal intensity, T1 map = T1 map method, v_e = volume of extravascular extracellular space, v_p = volume of vascular plasma space, WM = white matter

the B1 inhomogeneity can be revised, it takes some time and is not properly corrected, making it somewhat difficult for clinical practice [25,26]. On the other hand, the T1 map using the synthetic MRI method can be reproduced and has a reasonable scan time. Some studies recommend a fixed value method. According to Larsson et al. [27], the use of a fixed T1 is recommended when monitoring changes in parameters of DCE MRI in high-grade glioma patients, thereby simplifying the analysis of DCE MRI in a clinical setting. Conte et al. [28] reported that T1 mapping is not mandatory because it does not improve the diagnostic accuracy of DCE MRI for glioma grading, and the use of a fixed T1 value represents a valid alternative to T1 mapping for DCE MRI analysis [28]. However, these two studies did not suggest that the fixed value method is superior (or more efficient). What they meant was a fixed value method can be clinically useful as it could also carry stable and simple applications. If T1 mapping becomes more robust and simple than existing mapping methods, it will no longer be necessary to use the fixed value method clinically as it is currently used.

To calculate the quantitative DCE MRI kinetic parameters, the AIF needs to be defined. There have been many reports establishing the most reliable and accurate method to determine the optimal AIF, but several controversies remain, such as the AIF detection locations and methods [29-31]. We used the population-based AIF for measuring the pharmacokinetic parameters of DCE MRI because the main purpose of this study was to investigate the T1 measurement method-associated differences in DCE MRI

https://doi.org/10.3348/kjr.2020.1201

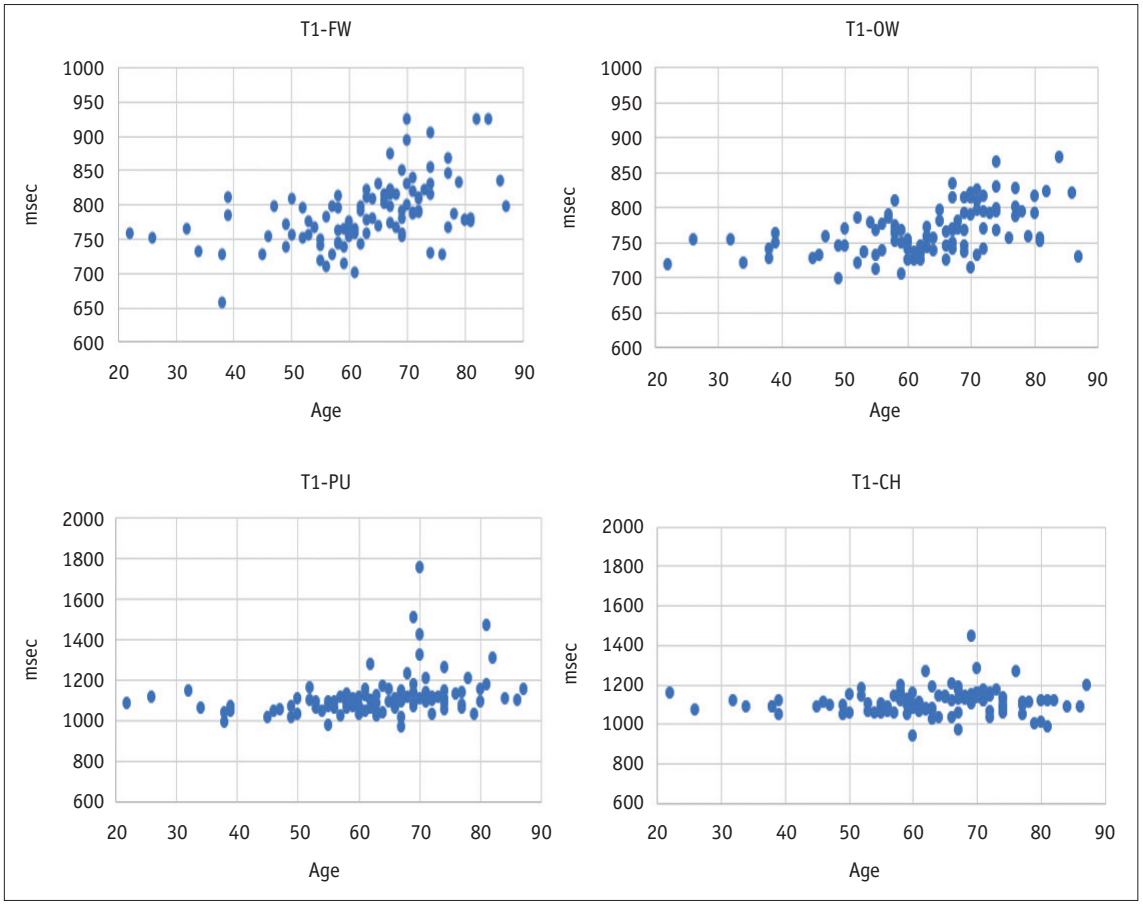

Fig. 7. Scatter plots showing correlation between the age and T1 values. The Pearson's *r* of the age and T1 values are: FW, 0.507 (p = 0.000); OW, 0.498 (p = 0.000); PU, 0.313 (p = 0.001); CH, 0.088 (p = 0.379). CH = caudate head, FW = frontal white matter, OW = occipital white matter, PU = putamen

Table 5. Comparison of the T1 Values between Male and Female

	Male	Female	Difference*	Mean Difference (%)†	*P*
Normal-appearing frontal WM	790	786	4	0.51	0.695
Normal-appearing occipital WM	769	765	4	0.52	0.650
Putamen	1126	1116	10	0.89	0.533
Caudate head	1105	1115	-10	-0.90	0.500

*Difference = male - female, †Mean difference = difference/male x 100. WM = white matter

parameters. An application of the population-based AIF could minimize the potential AIF-associated errors between the fixed value method group and the T1 map method group.

In this study, we obtained the pharmacokinetic parametric values in the normal-appearing frontal WM, normal-appearing occipital WM. Knowing the parametric values of DCE MRI in normal-appearing regions will provide a better understanding of brain diseases affecting brain-blood barrier permeability. Some studies revealed that the permeability changes measured by DCE MRI in brain lesions without visible contrast enhancement, such as small vessel disease [32-34]. The high signal intensity areas on pre-contrast FLAIR imaging have a longer T1 relaxation time than the normal WM, which requires the correction of the baseline T1 value for the DCE MRI. We also found that there were significant differences in the pharmacokinetic parameters between normal-appearing and high-signal intensity areas on FLAIR imaging. Therefore, we believe that our information can be used for future research on WM diseases.

There are some limitations to this study, in addition to the retrospective design. First, we did not use an automatic segmentation method for ROI selection. However,

https://doi.org/10.3348/kjr.2020.1201

Korean Journal of Radiology
KJR

the observers carefully drew the ROIs to minimize the location differences among subjects, and we chose brain regions that are visually definite areas. Second, we did not subclassify the high signal intensity lesions in the WM on FLAIR imaging, which could result from various WM affecting diseases, such as small vessel disease, interstitial edema, and demyelinating disease. However, we included non-enhancing lesions, so they could be categorized as inactive lesions, which did not cause significant differences in brain-blood barrier permeability. Third, our study did not include the diagnostic performances of the T1 map method in some specific diseases, including enhancing lesions, for which future studies are warranted.

In conclusion, we found that the pharmacokinetic parameters of DCE MRI in each brain region based on the T1 map method using synthetic MRI were significantly different from those using the fixed baseline T1 value, which could result from the application of the individual T1 values. In addition, the T1 map method also showed comparable interobserver agreements with the fixed baseline T1 value method for measuring the pharmacokinetic parameters of DCE MRI. We believe that the T1 map method using synthetic MRI may be helpful for reflecting individual differences and reliable measurements in clinical applications of DCE MRI.

Conflicts of Interest

The authors have no potential conflicts of interest to disclose.

Author Contributions

Conceptualization: Seung Hong Choi. Data curation: Seung Hong Choi. Formal analysis: Dong Jae Shin, Roh-Eul Yoo, Koung Mi Kang. Funding acquisition: Seung Hong Choi. Investigation: Dong Jae Shin, Sang Won Jo, Eun Jung Lee. Methodology: Seung Hong Choi, Tae Jin Yun, Ji-Hoon Kim, Chul-Ho Sohn. Project administration: Seung Hong Choi. Resources: Dong Jae Shin. Software: Dong Jae Shin, Koung Mi Kang. Supervision: Seung Hong Choi. Validation: Seung Hong Choi. Visualization: Dong Jae Shin. Writing—original draft: Dong Jae Shin. Writing—review & editing: Seung Hong Choi.

ORCID iDs

Dong Jae Shin
https://orcid.org/0000-0002-8044-6277
Seung Hong Choi
https://orcid.org/0000-0002-0412-2270
Roh-Eul Yoo
https://orcid.org/0000-0002-5625-5921
Koung Mi Kang
https://orcid.org/0000-0001-9643-2008
Tae Jin Yun
https://orcid.org/0000-0001-8441-4574
Ji-Hoon Kim
https://orcid.org/0000-0002-6349-6950
Chul-Ho Sohn
https://orcid.org/0000-0003-0039-5746
Sang Won Jo
https://orcid.org/0000-0002-9542-7378
Eun Jung Lee
https://orcid.org/0000-0002-2933-2995

REFERENCES

1. Gaddikeri S, Gaddikeri RS, Tailor T, Anzai Y. Dynamic contrast-enhanced MR imaging in head and neck cancer: techniques and clinical applications. *AJNR Am J Neuroradiol* 2015;37:588-595
2. Cheng HL. Investigation and optimization of parameter accuracy in dynamic contrast-enhanced MRI. *J Magn Reson Imaging* 2008;28:736-743
3. Tofts PS, Brix G, Buckley DL, Evelhoch JL, Henderson E, Knopp MV, et al. Estimating kinetic parameters from dynamic contrast-enhanced T(1)-weighted MRI of a diffusable tracer: standardized quantities and symbols. *J Magn Reson Imaging* 1999;10:223-232
4. Wang HZ, Riederer SJ, Lee JN. Optimizing the precision in T1 relaxation estimation using limited flip angles. *Magn Reson Med* 1987;5:399-416
5. Ogg RJ, Kingsley PB. Optimized precision of inversion-recovery T1 measurements for constrained scan time. *Magn Reson Med* 2004;51:625-630
6. Freeman AJ, Gowland PA, Mansfield P. Optimization of the ultrafast Look-Locker echo-planar imaging T1 mapping sequence. *Magn Reson Imaging* 1998;16:765-772
7. Haacke EM, Filleti CL, Gattu R, Ciulla C, Al-Bashir A, Suryanarayanan K, et al. New algorithm for quantifying vascular changes in dynamic contrast-enhanced MRI independent of absolute T1 values. *Magn Reson Med* 2007;58:463-472
8. Yun TJ, Park CK, Kim TM, Lee SH, Kim JH, Sohn CH, et al. Glioblastoma treated with concurrent radiation therapy and temozolomide chemotherapy: differentiation of true progression from pseudoprogression with quantitative dynamic contrast-enhanced MR imaging. *Radiology* 2015;274:830-840
9. Yu Y, Jiang Q, Miao Y, Li J, Bao S, Wang H, et al. Quantitative analysis of clinical dynamic contrast-enhanced MR imaging for evaluating treatment response in human breast cancer.

 https://doi.org/10.3348/kjr.2020.1201

Radiology 2010;257:47-55
10. Riederer SJ, Suddarth SA, Bobman SA, Lee JN, Wang HZ, MacFall JR. Automated MR image synthesis: feasibility studies. *Radiology* 1984;153:203-206
11. Warntjes JB, Dahlqvist O, Lundberg P. Novel method for rapid, simultaneous T1, T2*, and proton density quantification. *Magn Reson Med* 2007;57:528-537
12. Blystad I, Warntjes JB, Smedby O, Landtblom AM, Lundberg P, Larsson EM. Synthetic MRI of the brain in a clinical setting. *Acta Radiol* 2012;53:1158-1163
13. Kang KM, Choi SH, Hwang M, Yun TJ, Kim JH, Sohn CH. T1 shortening in the globus pallidus after multiple administrations of gadobutrol: assessment with a multidynamic multiecho sequence. *Radiology* 2018;287:258-266
14. Blystad I, Håkansson I, Tisell A, Ernerudh J, Smedby Ö, Lundberg P, et al. Quantitative MRI for analysis of active multiple sclerosis lesions without gadolinium-based contrast agent. *AJNR Am J Neuroradiol* 2016;37:94-100
15. Krauss W, Gunnarsson M, Andersson T, Thunberg P. Accuracy and reproducibility of a quantitative magnetic resonance imaging method for concurrent measurements of tissue relaxation times and proton density. *Magn Reson Imaging* 2015;33:584-591
16. Heye T, Davenport MS, Horvath JJ, Feuerlein S, Breault SR, Bashir MR, et al. Reproducibility of dynamic contrast-enhanced MR imaging. Part I. Perfusion characteristics in the female pelvis by using multiple computer-aided diagnosis perfusion analysis solutions. *Radiology* 2013;266:801-811
17. Wansapura JP, Holland SK, Dunn RS, Ball WS Jr. NMR relaxation times in the human brain at 3.0 tesla. *J Magn Reson Imaging* 1999;9:531-538
18. Gelman N, Ewing JR, Gorell JM, Spickler EM, Solomon EG. Interregional variation of longitudinal relaxation rates in human brain at 3.0 T: relation to estimated iron and water contents. *Magn Reson Med* 2001;45:71-79
19. Lu H, Nagae-Poetscher LM, Golay X, Lin D, Pomper M, van Zijl PC. Routine clinical brain MRI sequences for use at 3.0 Tesla. *J Magn Reson Imaging* 2005;22:13-22
20. Wright PJ, Mougin OE, Totman JJ, Peters AM, Brookes MJ, Coxon R, et al. Water proton T1 measurements in brain tissue at 7, 3, and 1.5 T using IR-EPI, IR-TSE, and MPRAGE: results and optimization. *MAGMA* 2008;21:121-130
21. Tanenbaum LN, Tsiouris AJ, Johnson AN, Naidich TP, DeLano MC, Melhem ER, et al. Synthetic MRI for clinical neuroimaging: results of the Magnetic Resonance Image Compilation (MAGiC) prospective, multicenter, multireader trial. *AJNR Am J Neuroradiol* 2017;38:1103-1110
22. Breger RK, Yetkin FZ, Fischer ME, Papke RA, Haughton VM, Rimm AA. T1 and T2 in the cerebrum: correlation with age, gender, and demographic factors. *Radiology* 1991;181:545-547
23. Steen RG, Gronemeyer SA, Taylor JS. Age-related changes in proton T1 values of normal human brain. *J Magn Reson Imaging* 1995;5:43-48
24. Cho S, Jones D, Reddick WE, Ogg RJ, Steen RG. Establishing norms for age-related changes in proton T1 of human brain tissue in vivo. *Magn Reson Imaging* 1997;15:1133-1143
25. Tietze A, Mouridsen K, Mikkelsen IK. The impact of reliable prebolus T_1 measurements or a fixed T_1 value in the assessment of glioma patients with dynamic contrast enhancing MRI. *Neuroradiology* 2015;57:561-572
26. Nam JG, Kang KM, Choi SH, Lim WH, Yoo RE, Kim JH, et al. Comparison between the prebolus T1 measurement and the fixed T1 value in dynamic contrast-enhanced MR imaging for the differentiation of true progression from pseudoprogression in glioblastoma treated with concurrent radiation therapy and temozolomide chemotherapy. *AJNR Am J Neuroradiol* 2017;38:2243-2250
27. Larsson C, Kleppestø M, Grothe I, Vardal J, Bjørnerud A. T1 in high-grade glioma and the influence of different measurement strategies on parameter estimations in DCE-MRI. *J Magn Reson Imaging* 2015;42:97-104
28. Conte GM, Altabella L, Castellano A, Cuccarini V, Bizzi A, Grimaldi M, et al. Comparison of T1 mapping and fixed T1 method for dynamic contrast-enhanced MRI perfusion in brain gliomas. *Eur Radiol* 2019;29:3467-3479
29. Li X, Cai Y, Moloney B, Chen Y, Huang W, Woods M, et al. Relative sensitivities of DCE-MRI pharmacokinetic parameters to arterial input function (AIF) scaling. *J Magn Reson* 2016;269:104-112
30. Rata M, Collins DJ, Darcy J, Messiou C, Tunariu N, Desouza N, et al. Assessment of repeatability and treatment response in early phase clinical trials using DCE-MRI: comparison of parametric analysis using MR- and CT-derived arterial input functions. *Eur Radiol* 2016;26:1991-1998
31. You SH, Choi SH, Kim TM, Park CK, Park SH, Won JK, et al. Differentiation of high-grade from low-grade astrocytoma: improvement in diagnostic accuracy and reliability of pharmacokinetic parameters from DCE MR imaging by using arterial input functions obtained from DSC MR imaging. *Radiology* 2018;286:981-991
32. Zhang CE, Wong SM, Uiterwijk R, Backes WH, Jansen JFA, Jeukens CRLPN, et al. Blood-brain barrier leakage in relation to white matter hyperintensity volume and cognition in small vessel disease and normal aging. *Brain Imaging Behav* 2019;13:389-395
33. Thrippleton MJ, Backes WH, Sourbron S, Ingrisch M, van Osch MJP, Dichgans M, et al. Quantifying blood-brain barrier leakage in small vessel disease: review and consensus recommendations. *Alzheimers Dement* 2019;15:840-858
34. Cramer SP, Simonsen H, Frederiksen JL, Rostrup E, Larsson HB. Abnormal blood-brain barrier permeability in normal appearing white matter in multiple sclerosis investigated by MRI. *Neuroimage Clin* 2013;10;4:182-189

https://doi.org/10.3348/kjr.2020.1201